AAPS PharmSciTech, Vol. 9, No. 1, March 2008 (© 2007)
DOI: 10.1208/s12249-007-9016-6

Research Article

Formulation and Evaluation of a Salted-out Isoniazid-loaded Nanosystem

Lisa C. du Toit,[1] Viness Pillay,[1] Yahya E. Choonara,[1] and Sunny E. Iyuke[2]

Received 9 May 2007; accepted 22 October 2007; published online 25 January 2008

Abstract. The purpose of this study was to develop a drug-loaded nanosystem that has the ability to achieve flexible yet rate-controlled release of model drug isoniazid (INH) employing either an aqueous or emulsion-based salting-out approach. Formulation conditions were aimed at reducing the polymeric size with subsequent rate-modulated INH release patterns from the polymeric nanosystem. The emulsion-based salted-out nanosystems had particle sizes ranging from 77–414 nm and a zeta potential of −24 mV. The dispersant dielectric constant was set at 78.5 and a conductivity of 3.99 mS/cm achieved. The reduced nanosystem size of the aqueous-based approach has demonstrated an intrinsically enhanced exposure of methacrylic acid-ethyl acrylate to zinc sulphate which was employed as a crosslinking reagent. This resulted in robustly interconnected polymeric supports in which INH was efficiently embedded and subsequently released. The multi-layer perceptron data obtained showed that the aqueous and emulsion-based salting out approaches had Power (law) (MSE=0.020) and Linear (MSE=0.038) relationships, respectively. Drug release from the nanosystems occurred in two phases with an initial burst-release in aqueous-based nanosystems (30–100%) and significantly lower bursts observed in emulsion-based nanosystems (20–65%) within the first 2 h. This was followed by a gradual exponential release phase over the remaining 12 h. The nanosystems developed demonstrated the ability to control the release of INH depending on the formulation approach adopted.

KEY WORDS: crosslinking; drug release; methacrylic acid-ethyl acrylate; nanoparticles; tuberculosis.

INTRODUCTION

The current surge of interest in nanoparticulate-based anti-tuberculosis (TB) drug delivery systems is increasing and perhaps pertinently applicable to developing countries and the rest of Africa since TB infection is facing a momentous incline inextricably linked to escalating cases of HIV infection. Concurrently, isoniazid (INH), which is a front-line antimicrobial in TB therapy, has hepatotoxic complications that range in severity from asymptomatic elevation of serum transaminases to hepatic failure that sympathetically requires liver transplantation. Therefore, the technological advantages in using nanoparticle-based INH delivery that is able to enhance the bioavailability of INH would make TB treatment an attractive option as much less drug would be needed, thus significantly reducing side-effects (1–3).

Nanoparticulate systems can be designed to allow flexible yet rate-modulated INH release from co-polymers matrices such as methacrylic acid-ethyl acrylate (MAEA). Such systems that can be administered once-daily in a single dose and maintain drug levels for longer durations could serve to improve the bioavailability of anti-TB agents, reduce the dose frequency and duration of treatment, reduce the inherent toxicity of TB treatment, achieve localised drug delivery to a designated region of the body owing to the nano-sized particles, optimised drug absorption, and may thus resolve the problem of non-adherence to prescribed therapy, which is one of the major obstacles in the control of TB epidemics (4).

Nanoparticles are able to enhance drug for purposes of optimised deposition to targeted tissues with surface modifications that are able to mediate drug targeting as well as reduce cytotoxicity by employing preferential binding to target tissues. The cytotoxicity of co-polymeric biocompatible nanoparticles as drug carriers for pulmonary application was previously investigated *in vitro* on primary airway epithelium cells and the cell line 16HBE14o. The uptake of nanoparticles into cells was examined by confocal laser scan microscopy and flow cytometry. Cytotoxicity was evaluated by an LDH-release-test and the inflammatory potential of the polymeric nanoparticles was assessed by measuring IL-8 release. Results showed that the nanoparticles provoked little or no cytotoxicity and no inflammation as measured by IL-8 release. Based on the low cytotoxicity and inflammatory potential in combination with an efficient uptake in human bronchial epithelial cells, polymeric nanoparticles were deemed suitable drug carriers for pulmonary application (4).

Formulation approaches of nanoparticles for pharmaceutical use are divided broadly into two categories based on the physicochemical interactions such as phase separation and solvent evaporation, and on chemical reactions such as polymerisation and polycondensation of synthetic monomers (5,6).

[1] Division of Pharmaceutics, Department of Pharmacy and Pharmacology, University of the Witwatersrand, 7 York Road, Parktown, 2193 Johannesburg, South Africa.
[2] School of Chemical and Metallurgical Engineering, University of the Witwatersrand, P/Bag 3, Wits, 2050 Johannesburg, South Africa.
[3] To whom correspondence should be addressed. (e-mail: viness.pillay@wits.ac.za)

The former approach has been often adopted for the preparation of nanoparticles prepared from hydrophobic or crosslinked water-insoluble hydrophilic polymers such as polylactic acids, celluloses, polyacrylates, and polymethacrylates (3).

Considering the preparation of nanoparticles for oral administration, properties such as the size and nature of the polymer used to manufacture the particles play a critical role in the rate of uptake from the intestinal tract. These properties are often influenced by the preparation approach, selected in accordance with the drug and polymer employed, while the ultimate physicochemical properties of the particles are critically influenced by the conditions of manufacturing. However, control of the particle size is commonly inadequate in size-reduction approaches, as the achievable particle size depends on the physicochemical properties of the material in particular the hardness and thermal properties. Furthermore, in order to achieve nano-sizes, the processing times may be extended, ranging up to several days, thereby increasing the risk of chemical or microbiological contamination. It has also been shown that high-energy milling procedures, which are commonly required to achieve small particle sizes, can lead to uncontrollable crystal damage (5).

The aim of this study was therefore to develop a method to overcome the limitations associated with previous nanoparticulate drug delivery system formulations, thereby combining the advantages of nanoparticles as a mode of drug delivery with the added benefits of the pH-sensitive salted-out MAEA polymer been employed. The concept of site-specific (pulmonary) controlled drug release is reiterated for the nano-enabled drug delivery system developed in this study, referred to throughout as the "nanosystem" owing to the distinctive advantages over classical methods of drug delivery, emerging from the need for effective management of TB. This study implements the technology in two comparative salting-out *in vitro* methodological approaches for the formulation of the anti-TB nanosystem, incorporating INH. The aqueous and emulsion-based salting-out approaches were compared mathematically using a multilayer perceptron (MLP) neural network simulation with one hidden layer, a SigmoidAxon transfer function and ConjugateGradient learning rule (7–10,12).

MATERIALS AND METHODS

Materials

Methacrylic acid-ethyl acrylate copolymer (MAEA), (Eudragit® L100-55), sodium lauryl sulphate and polysorbate 80 were obtained from Röhm Pharma Polymers (Röhm GmbH, Darmstadt, Germany). Isoniazid (INH) was purchased from Aldrich® (Sigma-Aldrich Inc., St. Louis, USA). Sodium carboxymethylcellulose (NaCMC), sodium hydroxide (NaOH) and zinc sulphate ($ZnSO_4$) was purchased from Saarchem (Wadeville, Gauteng, South Africa). All other solvents and reagents were of analytical grade and were used as received.

Table I. Formulation of Nanosystems by an Emulsion-based Salting-out Approach

Formulation Components	Concentration (% *w/w*)
Organic phase	
MAEA	10.00
INH	2.00
Organic solvent (acetone)	88.00
Aqueous phase	
NaCMC (colloidal stabiliser)	5.00
$ZnSO_4.7H_2O$	41.31
Double deionised water qs.	100.00
Stirring speed (rpm)	800–2000

Table II. Formulation of Nanosystems by an Aqueous-based Salting-out Approach

Formulation Components	Quantity (g)
Aqueous dispersion (NP suspension)	
30% *w/w* latex	50.00
INH	6.00
Electrolyte solution	
$ZnSO_4.7H_2O$	41.31
Concentrated HCl qs.	pH 2
Double deionised water qs.	100.00

Methods

Preparation of the Nanosystem by an Emulsion-based Salting-out Approach

MAEA, NaCMC, $ZnSO_4$ and INH were used as the polymer, viscosity-enhancing agent, crosslinking electrolyte and model drug, respectively, as per compositions listed in Table I. NaCMC was included to potentially improve drug release in macrophages (11–14). An aqueous solution of NaCMC (50 g) was added under agitation (Heidolph® propeller stirrer, Labotec, Gauteng, South Africa) to an organic solution of MAEA and INH resulting in an o/w emulsion. Thereafter, 50 ml deionised water was added to allow diffusion between the two phases that led to INH-loaded nanosystem formation. The nanosystems were purified with deionised water, collected by centrifugation and lyophilized for 12 h (Virtis Lyophilizer, Virtis®, Gardiner, NY, USA), which was sufficient to obtain a free-flowing powder, without extensive particle agglomeration, and maintenance of pre-lyophilisation morphology.

Preparation of the Nanosystem by an Aqueous-based Salting-out Approach

The nanosystem was prepared in accordance with the formulation compositions listed in Table II. This synthetic approach followed re-dispersal of MAEA to a latex comprising an aqueous dispersion of MAEA affected by the addition of 1M NaOH, to neutralize 6 mole% of the carboxyl groups, and achieve a colloidal aqueous dispersion of even sized polymeric particles (15–17). INH was dissolved in the polymeric solution to obtain a MAEA/INH ratio of 5:1. The experimental set-up for the atomization process is depicted in Fig. 1. Briefly, 10 ml of drug-loaded latex was pumped through an atomizer with a feed rate adjusted to approximately 1–10 ml/min through a spray nozzle (internal diameter = 1 mm). Compressed air was injected to disperse the latex into a stainless steel vessel containing 200 ml of a 41.31% *w/v* $ZnSO_4$ crosslinking solution which induced the formation of aerosol-

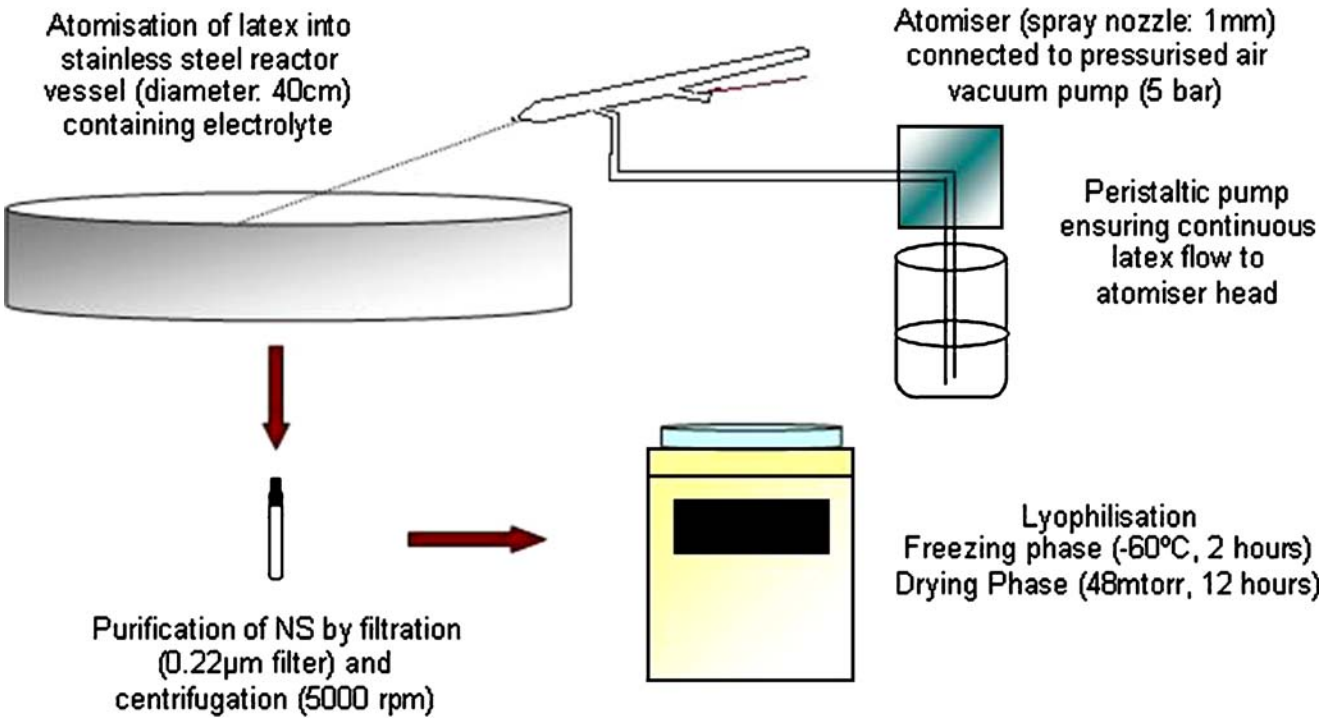

Fig. 1. Production sequence set-up for the novel aqueous salting-out and spray atomisation for the nanosystem preparation

ized droplets into INH-loaded salted-out nanosystems. The nanosystems were incubated in the reactor solution for 60 minutes to allow formation of discrete and compact nanosystems, purified with deionised water, and lyophilized as previously described. The morphological architecture and IR spectra of the nanosystem were evaluated for elucidating the assemblage and physicochemical and physicomechanical properties (18–20).

Vibrational Transitions in the Nanosystem Determined by Fourier Transform Infra-Red Analysis

Fourier transform infra-red (FTIR) analysis was performed on the MAEA nanoparticles formulated employing both approaches. Samples of 20 mg were triturated with 2 g potassium bromide and then compressed under a pressure of 8 tons in a 13 mm die to produce a disk. Infrared spectra of the respective nanosystems were determined from KBr discs using an infrared spectrophotometer (Nicolet Analytical Instruments) at a scanning range between 4000–400 cm^{-1}.

Characterization of Particle Morphology, Size and Zeta Potential

The surface morphology of the nanosystem architectures were analysed employing scanning electron microscopy (SEM; 840 SEM, JEOL, Japan) and the particle size and zeta potential was determined using photon correlation spectroscopy (PCS) on a Zetasizer Nano ZS instrument (Malvern Instruments, Worcestershire, UK). Briefly, for the particle size and zeta potential measurements samples were diluted with deionized water at 25 °C with a dispersant dielectric constant value of 78.5. The zeta potential was measured based on the Smoluchowski diffusion equation (21, 22). SEM samples were prepared by gently dipping on a copper grid and sputter-coated with carbon and gold-palladium shadowing. Different magnifications at 10 keV were selected to view the overall and in-depth surface structure to qualitatively elucidate factors such as the degree of chain entanglement and network density.

Plackett–Burman Experimental Screening Design for Critical Factor Identification

The factor settings for the nanosystem formulations originating from both salting-out approaches are shown in

Table III. Plackett–Burman Design for the Emulsion-based Salted-out Nanosystems

Formulation	[Polymer] (% *w/v*)	Polymer/Drug Ratio	Processing Temperature (°C)
1	15	20	20
2	15	20	20
3	5	20	20
4	10	11	50
5	5	2	80
6	5	20	80
7	15	2	80
8	15	2	20
9	5	20	80
10	5	2	20
11	15	2	80
12	10	11	50
13	15	20	80
14	5	2	20

Table IV. Plackett–Burman Design for the Aqueous-based Salted-out Nanosystems

Formulation	[Polymer] (% *w/v*)	Polymer/Drug Ratio	Salt Solution Acidification (pH)
1	10	11	3.50
2	5	20	5.50
3	15	2	1.50
4	5	2	5.50
5	5	2	1.50
6	15	2	5.50
7	15	20	1.50
8	5	2	1.50
9	10	11	3.50
10	15	20	1.50
11	5	20	5.50
12	15	20	5.50
13	5	20	1.50
14	15	2	5.50

Tables III and IV. The design employed a single central point with the independent formulation variables encompassing the polymer concentration, polymer/drug ratio and the acidification pH of the electrolyte solutions employed. The responses measure were the drug incorporation efficiency (DIE %) and the nanosystem yield value (%) for both the emulsion and aqueous-based salted-out nanosystems. The polymer concentrations (in polymer solution or dispersion), which ranged from 3–15% *w/v*, were prepared from the 30% *w/w* stock solution by dilution in deionised water.

Analysis of Nanosystem Recovery

Nanosystem recovery was analysed to determine the quantity of drug-loaded nanoparticles that were obtained from the initial starting material employed during the formulation, which may also be referred to as the yield (%) using Equation 1. The individual values for three replicate determinations with mean values were ascertained. The initial mass was the mass of the total formulation components.

$$\text{Recovery\_}(\%) = \frac{\text{Mass}_{\text{recovered}}}{\text{Mass}_{\text{initial}}} \times 100 \quad (1)$$

Determination of the Drug Incorporation Efficiency of the Nanosystem

Samples of the lyophilized nanosystem were accurately weighed and dissolved in PBS pH 7.0 by centrifugation. Five milliliters aliquots were filtered through a 0.22 μm filter (Millipore Corporation, Bedford, MA, USA) to remove any insoluble polymer residues. The filtered samples were centrifuged (5,000 rpm for 60 min) and the supernatant was sampled. Drug incorporation efficiency (DIE) was determined spectrophotometrically at 263 nm using linearity curves (R^2=0.99) and 1instituting Eq. 2:

$$\text{DIE\_}(\%) = \frac{\text{Drug}_{\text{actual}}}{\text{Drug}_{\text{Theoretical}}} \times 100 \quad (2)$$

In Vitro Drug Release Studies

Drug release studies were undertaken at a neutral pH (PBS pH 7.0) on all formulations. 10 mg of each formulation were accurately weighed and dispensed into specimen bottles of 25 ml capacity containing 20 ml of PBS. The bottles were secured and agitated in a shaker bath (Labex, Stuart SBS40®, Gauteng, South Africa) maintained at 37.5±0.5 °C. Agitation was discontinued 1 minute prior to sampling to allow the nanosystem to settle and thus to minimise the quantity of intact particles removed from the dissolution milieu. All aliquots withdrawn were subjected to centrifugation and appropriately diluted prior to UV spectrophotomeric analysis at 263 nm. Experiments were performed in triplicate on all formulations.

RESULTS AND DISCUSSION

Particle Morphology, Size, Zeta Potential and Vibrational Transitions

The morphology and overall architecture of the resultant particles could be best described as drug nanoparticles embedded in a polymeric micro- or nano-matrix support (Figs. 2 and 4). SEM imaging of the nanosystems revealed the presence of sphere-like particles with particle sizes ranging from 77.08–414.1 nm as confirmed by measurements performed on a Zetasizer Nano ZS instrument (two to four measurements of three separate batches). Particle size characterization results of the nanosystems were in agreement with the SEM images. Zeta potential measurements indicated a mean value of −24 mV at a count rate of 2,662.2 kcps with a maximum of 12 zeta runs. The result quality was superior with a conductivity of 3.99 mS/cm (Fig. 3a and b).

SEM analysis revealed that nanoparticles were INH-loaded which was confirmed by FTIR spectroscopy. Nanosystems formulated via the emulsion-based salting-out approach had a more compact architecture and a mean diameter of 166.50±23.33 nm while those formulated by the aqueous-based salting-out approach had a flattened, porous architecture (mean density, 0.266±0.072 g/cm^3), which would be aerodynamically conducive to aerosol delivery and facilitated a tubular morphological transition in PBS (Fig. 4). The mean diameter of the preliminary form was 271.25±54.52 nm.

Nanoparticle formation by salting-out (nano-precipitation) employing emulsification and aqueous diffusion was associated with polymeric chain interactions at the polymeric droplet interface that involved a reduction in the interfacial tension and mechanical stabilization of the nanoparticles in the bulk electrolyte solution (hydrodynamic stabilization).

FTIR analysis of the nanosystems revealed the characteristic resonance and ionisation of the carboxylic acid group as a decreased band intensity between 1,680 and 1,725 cm^{-1}. When ionisation occurred, with formation of the COO^- group, resonance was possible between the two C–O bonds. As a consequence, the characteristic pendant anhydride absorption is replaced by the band in the 1,550–1,556 cm^{-1} region indicative of a degree of ionisation and cross-linking in the nanosystems and the presence of INH. The physicochemical characteristics of both salted-out nanosystems were comparable.

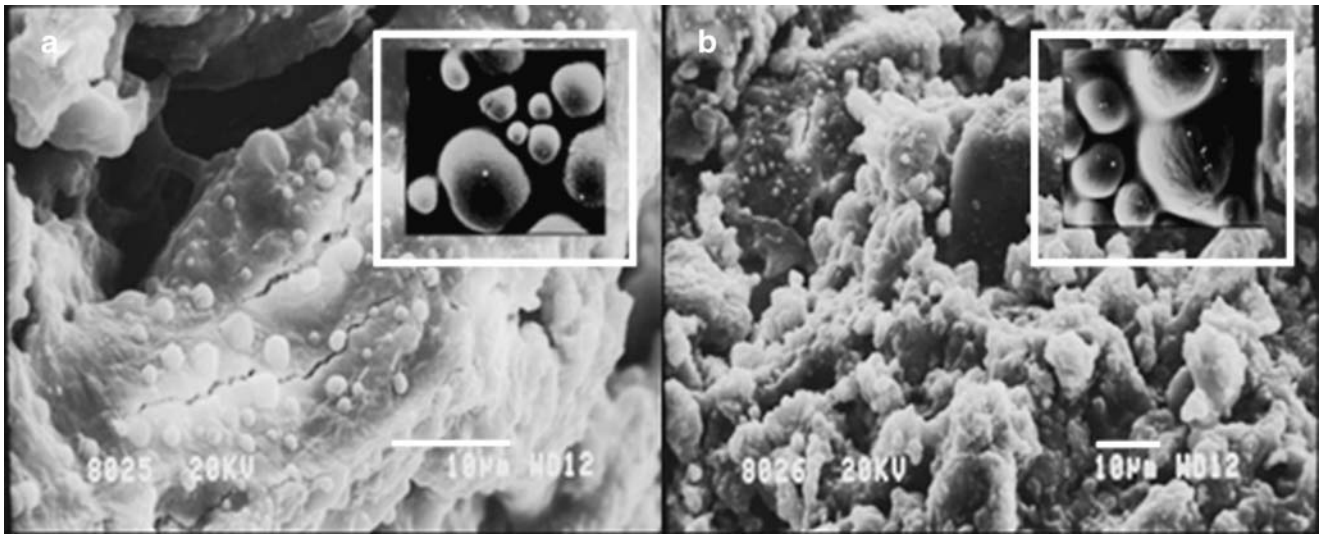

Fig. 2. SEM images of nanosystems formulated by **a** the emulsion-based salting-out and **b** the aqueous-based salting-out approaches depicting nanospheres embedded the polymeric micromatrix support

Particle size analysis was determined from SEM images of formulations to elucidate and estimate the size distribution yielded by each formulation approach. A reduction in the polymer concentration employed for nanosystem manufacture in the experimental designs dramatically reduced the mean diameters of the formulations. Emulsion-based salted-out nanosystems had mean diameters ranging from 4.89±0.33 nm to 43.46±28.06 nm and aqueous-based salted-out nanosystems ranged between 14.59±3.48 nm to 27.22±5.67 nm.

INH nanoparticles maintained a constant size distribution for each formulation approach. Emulsion-based salted-out nanosystems had mean diameters of 638.33±169.75 nm while aqueous based salted-out nanosystems were 466.5±144.27 nm. Nanosystem recovery was satisfactory for the investigated formulation approaches. The DIE values obtained for the aqueous-based formulations were lower, with the most favourable results obtained at higher polymer:drug ratios (20:1). Lower DIE values were attributable to the water-soluble nature of INH, leading to rapid partitioning into the aqueous electrolyte phase and lower quantities were entrapped during polymer phase separation. The larger surface area of the nanosystem also contributed to the loss of INH during fabrication.

In Vitro Drug Release Behaviour from the Nanosystem

Drug release from the nanosystem occurred in two phases with an initial burst-release of approximately 30–100% in aqueous-based formulations and 20–65% in emulsion-based formulations within the first 2 h. This was followed by a slower exponential release phase of drug over the remaining 12 h. The rapid initial release of INH was due to drug embedded close to the surface of the nanosystem matrix and the inherent large surface-to-volume ratio of the nanosystem architecture due to size. In most formulations, the interwoven architecture controlled drug release for upto 12 h. The measured responses emanating from the Placket Burman generated formulations and drug release is represented in Table V, and Figs. 5 and 6.

The erosional behaviour of the nanosystem prepared by the aqueous-based salting-out approach can be described by a tubular morphological transition after incubation for at least 6 h in PBS, which coincided with the final drug release phase observed in most formulations commencing between 6 and 12 h (Fig. 5). This is consequential of possible crystal growth and zinc oxide formation upon significant reaction of zinc cations with hydroxyl groups within the alkaline medium and the nanosystem architecture. The ZnO nuclei have been demonstrated to express a short rod- or prism-like form. This induces folding, and assumption of a tube-like configuration of the flattened matrix, which facilitates complete drug

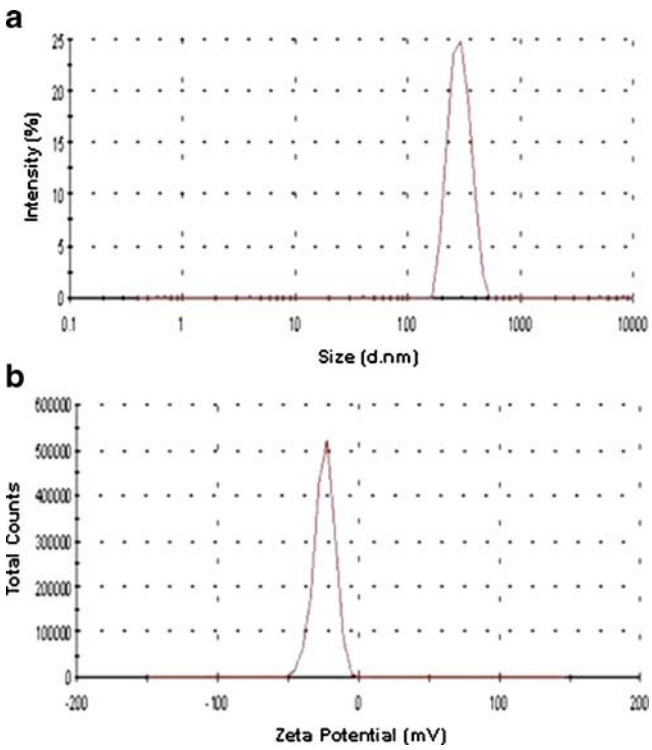

Fig. 3. Typical intensity plots obtained from particle characterization studies of **a** mean particle size (*Z*-average) and **b** mean zeta potential

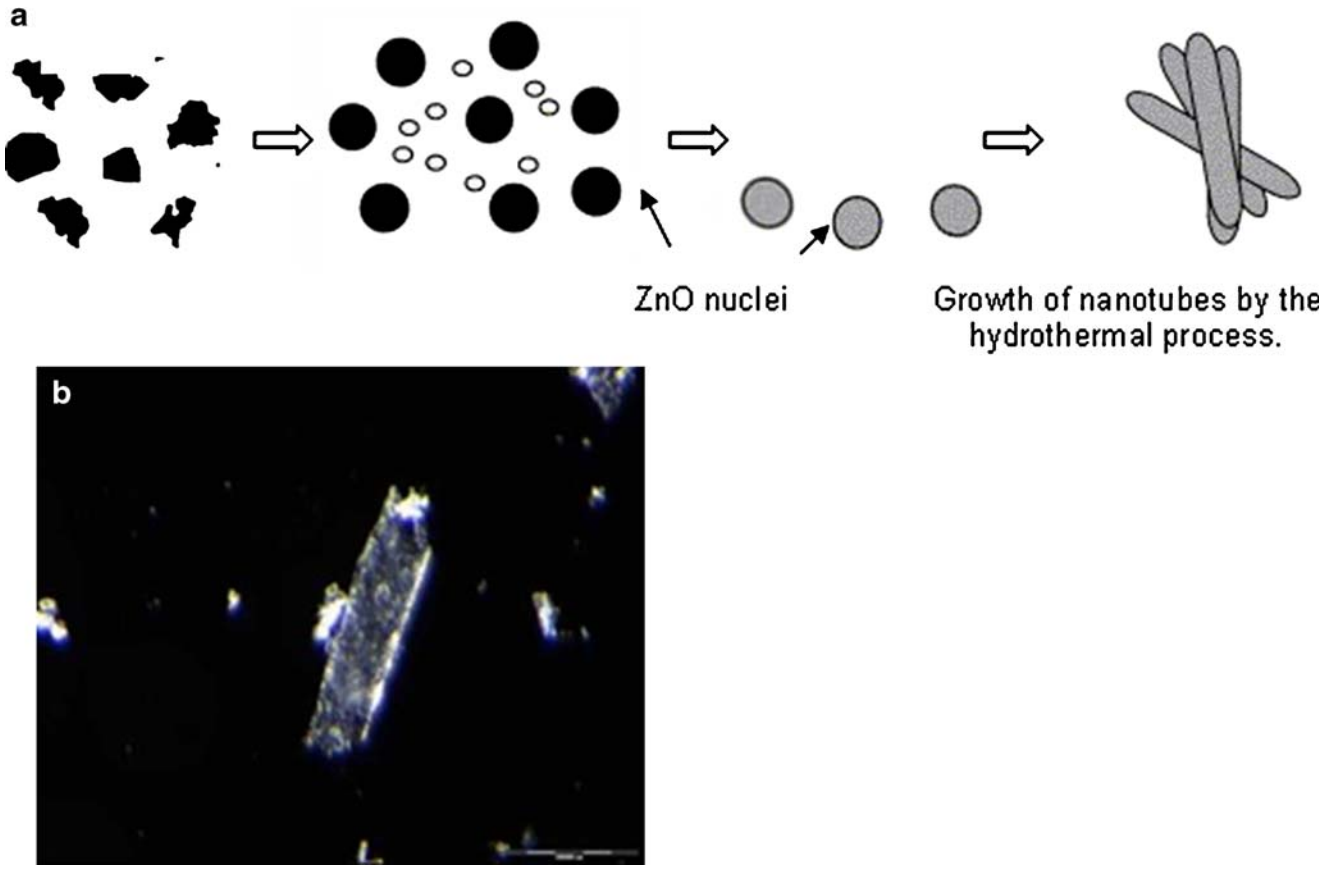

Fig. 4. **a** Schematic of zinc oxide crystal formation and **b** SEM depicting tubular transitions of nanosystems fabricated by the aqueous-based salting-out approach

dissolution. This architectural mobility can facilitate clearance following delivery of the drug.

Analysis of the Plackett–Burman Screening Design

Analysis of the Placket–Burman design generated for the emulsion-based salting-out approach identified that increases in the polymer concentration ($p=0.037$) and the processing temperature ($p=0.004$) significantly improved the yield. DIE within the polymeric matrices was significantly enhanced by increases in the polymer/drug ratio ($p=0.022$) and processing temperature ($p=0.031$). Effects of formulatory factors on nanosystem outcomes are represented in the response surface plots (Fig. 6).

The processing temperature notably affected drug release at 6 h, with lower quantities of drug being released when higher processing temperatures were employed (Fig. 6a). The advantageous effects in all cases of elevated processing temperatures can be attributed to the promotion of rapid elimination of the organic solvent to form compact polymeric matrices that efficiently embedded the drug within interconnected structures and controlled drug release to a greater extent.

Analysis of the Placket–Burman design generated for the aqueous salting-out approach identified the polymer/drug ratio as the only factor that significantly affected the nanosystem yield ($p=0.023$). DIE was improved by increasing the polymer:drug ratio, however, increasing the dilution of the MAEA copolymer essentially improved the DIE (Fig. 6b), possibly due to enhanced molecular dispersal of the drug amongst the polymeric chains during formulation. The burst release of INH at 0.5 h (40–50%) was notably reduced by

Table V. Measured Yield and Drug Incorporation Efficiency for Plackett–Burman Generated Formulations

	Emulsion Salted-Out NS		Aqueous Salted-Out NS	
Formulation No.	Yield (%)	DIE (%)[a]	Yield (%)	DIE (%)[b]
1	25.67	64.89	56.60	15.00
2	24.39	61.65	63.05	18.48
3	98.51	86.26	43.89	8.82
4	84.45	75.83	26.67	7.28
5	135.53	66.04	13.60	0.85
6	116.41	87.38	15.76	3.03
7	76.22	69.98	17.78	5.31
8	51.47	63.97	23.51	2.55
9	96.30	72.28	20.99	4.73
10	30.21	10.67	23.23	6.51
11	73.67	67.64	54.99	9.42
12	90.67	81.42	38.24	8.21
13	66.96	184.96	56.78	9.56
14	33.68	11.90	30.39	6.75

[a] For Emulsion Salted-Out NS Analysis: S.D.: DIE $\leq 1.076\%$
[b] For Aqueous Salted-Out NS analysis: S.D.: DIE $\leq 4.29\times10^{-3}$ %

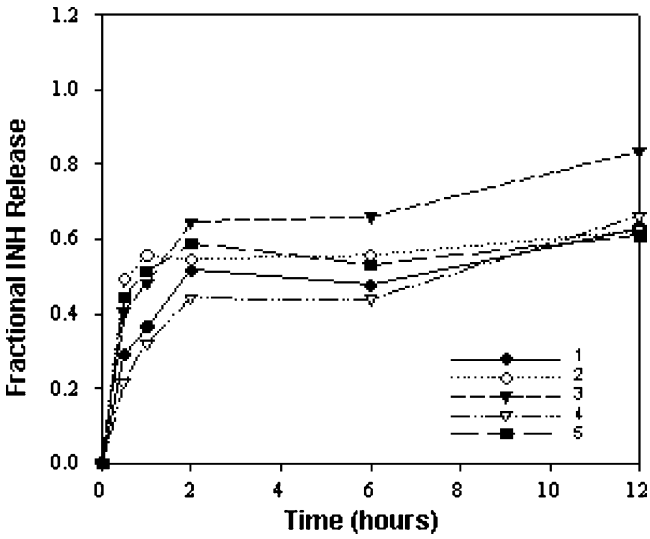

Fig. 5. Drug release profiles from aqueous-based salted-out nanosystem formulations in phosphate-buffered saline (PBS) pH 7.0

increasing the polymer concentration and polymer:drug ratio in the formulation (20–30%). The yield and DIE increased with a subsequent decrease of the burst release of INH at 0.5 h occurred with an increase in the polymer/drug ratio.

A more acidic pH of the salting-out and crosslinking solution adversely affected the DIE and drug release. This is purported to be a result of less efficient incorporation of INH nanoparticles in the polymeric micromatrices due to a rapid rate of MAEA coalescence in the highly protonated electrolyte solution, and a consequentially higher degree of surface deposition of drug.

Multi-layered Perceptron Neural Networks Simulation

Multi-layer perceptron (MLP) nets were used to train the multi-variable and chaotic experimental data obtained. The outputs correlated with the experiments and the multi-variable dependence on the INH release as proposed in Eqs. 3 and 4 for aqueous and emulsion salting out, respectively. The correlations of the models with the experimental data have reasonably low mean square errors of 0.020 and 0.038 for the aqueous and emulsion salting-out nanosystems, respectively.

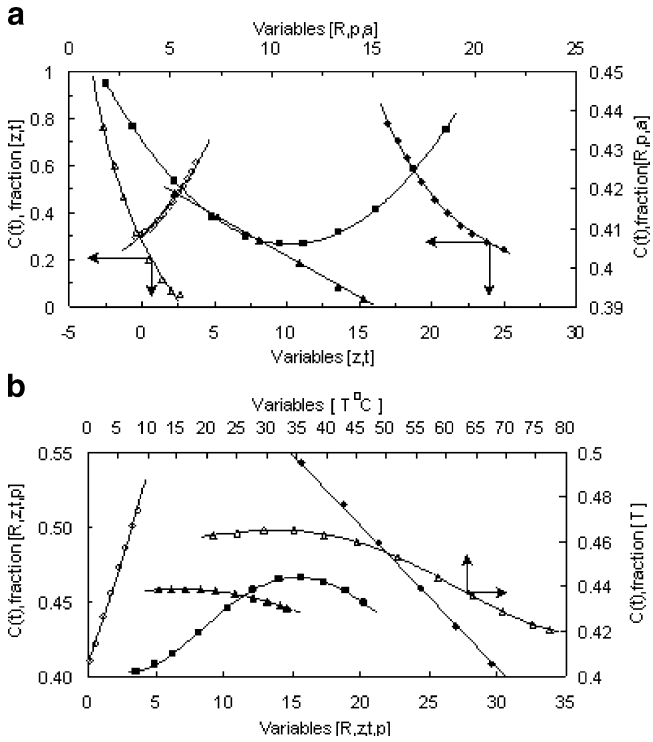

Fig. 7. Multi-variable effects on isoniazid release profiles. **a** Aqueous based-salting-out nanosystems **b** emulsion-based-salting-out nanosystems

The application of the MLP nets on the experimental data using a multi-variable model showed that all factors were observed to have significantly impacted the release of INH from aqueous and emulsion-based salting out. The corresponding least square correlation equations obtained are also presented in Fig. 7. Of particular interest as highlighted earlier is the effect of the nanosystem sizes on the INH release, where the aqueous and emulsion-based salting-outs have power and linear relationships, respectively as shown in Eqs. 3 and 4:

$$C(t)_{\text{aqueous}} = 4,923.4z^{-3.0865} \tag{3}$$

$$C(t)_{\text{emulsion}} = 0.0095z + 0.6915 \tag{4}$$

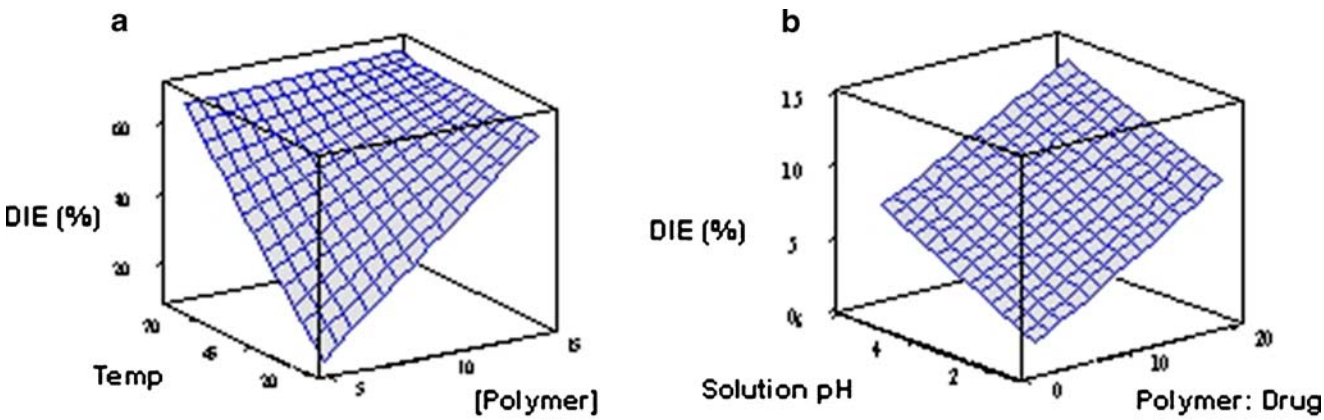

Fig. 6. Surface plots derived from the Placket Burman design for **a** emulsion-based nanosystems and **b** aqueous-based nanosystems

Where $C(t)$ represents the INH released and a function z for the size of the nanosystem. The difference in Eqs. 3 and 4 in terms of the effect of size on INH release, showed that an increased release of INH occurred as the nanosystem size decreased and was more prominent in the aqueous-based salting-out that in emulsion-based salting-out approach. In other words, while the INH release decreased exponentially of the nanosystem size in the aqueous-based-salting-out, the release decreased linearly with the emulsion-based-salting-out approach. This was a remarkable difference observed in the two approaches investigated for nanosystem fabrication.

The major advantage of the two salting-out methods employed in this study is the avoidance of chlorinated solvents and surfactants commonly used with conventional solvent evaporation approaches. The emulsion-based salting-out procedure is focused on the incorporation of an electrolyte-saturated aqueous solution comprising sodium carboxymethylcellulose, as opposed to the more commonly employed polyvinyl alcohol (PVA) as a viscosity-enhancing agent and stabiliser, into an acetone solution of the polymer (and drug) to form an oil-in-water emulsion. Suitability of the emulsion-based approach employed in this study to the applicable polymer and drug is assured due to adequate solubility in the designated polar solvents.

CONCLUSION

The aqueous-based salted-out nanosystem had a porous, flattened architecture and underwent a tubular morphological transition that pivotally coincided with complete drug release that may be viable for lung clearance and conducive to site-specific controlled release (23). MLP analysis has confirmed the rapid INH release in the aqueous-salting-out approach, as the nanosystem reduced into nanoscale sizes in accordance with Ficks Law of diffusion signifying that the nanosystem fabrication conditions aimed at reducing the polymeric size displayed promising INH release. The reduced size has also seen an intrinsically enhanced exposure of MAEA to the salting-out $ZnSO_4$ electrolyte, which resulted in a robustly interconnected polymeric support that efficiently embedded INH particles.

REFERENCES

1. A. S. Gelperina, I. N. Khalansky, Z. S. Skidan, A. I. Smirnova, S. E. Bobruskin, B. Severin, and F. E. TurowskiToxicological studies of doxorubicin bound to polysorbate 80-coated poly (butyl cyanoacrylate) nanoparticles in healthy rats and rats with intracranial glioblastoma. *Toxicol. Let* **126**:131–114 (2002).
2. S. Sakuma, M. Hayashi, and M. Akashi. Design of nanoparticles composed of graft copolymers for oral peptide delivery. *Adv. Drug Del. Rev* **47**:21–37 (2001).
3. M. J. Blanco Prieto, F. Delie, E. Fattal, A. Tartar, F. Puisieux, A. Gulik, and P. Couvreur. Characterization of V3 BRU peptide-loaded small PLGA microspheres prepared by a $(w_1/o)w_2$ emulsion solvent evaporation method. *Int. J. Pharm* **111**:137–145 (1994).
4. M. Brzoska, K. Langer, C. Coester, S. Loitsch, T. O. F. Wagner, and C. V. Mallinckrodt. Incorporation of biodegradable nanoparticles into human airway epithelium cells—*in vitro* study of the suitability as a vehicle for drug or gene delivery in pulmonary diseases. *Biochem. Biophys. Res. Commun* **318**no. 2, 562–570 (2004).
5. A. Sergio, G. Rodríguez, F. Puel, S. Briançon, E. Allémann, E. Doelker, and H. Fessi. Comparative scale-up of three methods for producing ibuprofen-loaded nanoparticles. *Eur. J. Pharm. Sci* **25**:357–367 (2005).
6. R. Allémann, E. Gurny, and E. Doelker. Preparation of aqueous polymeric nanodispersions by a reversible salting-out process: influence of process parameters on particle size. *Int. J. Pharm* **87**:247–253 (1992).
7. A. P. Tinke, K. Vanhoutte, R. MaesschalckDe, S. Verheyen, and H. WinterDe. A new approach in the prediction of the dissolution behaviour of suspended particles by means of their particle size distribution. *J. Pharm. Biomed. Anal* **39**:900–907 (2005).
8. C. G. Looney. *Pattern recognition using neural networks: Theory and algorithms for engineers and scientists*, Oxford University Press, Oxford, 1997, pp. 5–45.
9. E. Frias-Martinez, A. Sanchez, and J. Velez. Support vector machines versus multi-layer perceptrons for efficient off-line signature recognition. *Eng. Appl. Art. Intel* **19**:693–704 (2006).
10. M. S. Gibbsa, N. Morgan, H. R. Maier, G. C. Dandy, J. B. Nixon, and M. Holmes. Investigation into the relationship between chlorine decay and water distribution parameters using data driven methods. *Math. Comp. Model* **44**:485–498 (2006).
11. H. Demuth and M. Beale. Neural network toolbox for use with MATLAB®. *MathWorks Inc. Natick Mass* **3–1**:3–22 (1994).
12. M. P. Barrow, N. J. Tower, R. Taylor, and T. Drewello. Matrix-assisted laser-induced gas-phase aggregation of C_{60} oxides. *Chem. Phys. Let* **293**:302–308 (1998).
13. M. Gevrey, I. Dimopoulos, and S. Lek. Two-way interaction of input variables in the sensitivity analysis of neural network models. *Ecol. Model* **195**:43–50 (2006).
14. T. Cai and Z. Hu. Synthesis and self-assembly of nearly monodisperse nanoparticles of a naturally occurring polymer. *Langmuir* **20**:7355–7359 (2004).
15. Z. Cui, P. R. Lockman, C. S. Atwood, C. H. Hsu, A. Gupte, D. D. Allen, and R. J. Mumper. Novel D-penicillamine carrying nanoparticles for metal chelation therapy in Alzheimer's and other CNS diseases. *Eur. J. Pharm. Biopharm* **59**:263–272 (2005).
16. G. Liu, M. R. Garrett, P. Men, X. Zhu, G. Perry, and M. A. Smith. Nanoparticle and other metal chelation therapeutics in Alzheimer disease. *Biochimica et Biophysica Acta* **1741**:246–252 (2005).
17. S. De, and D. H. Robinson. Particle size and temperature effect on the physical stability of PLGA nanospheres and microspheres containing bodipy. *AAPS PharmSciTech*. **5**(4) (2004), Article 53.
18. A. Zahoor, S. Sharma, and G. K. Khuller. Inhalable alginate nanoparticles as antitubercular drug carriers against experimental tuberculosis. *Int. J. Antimicrob. Agents*. **26**:4298–303
19. R. Pandey, Z. Ahmad, S. Sharma, and G. K. Khuller. Nano-encapsulation of azole antifungals: potential applications to improve oral drug delivery. *Int. J. Pharm* **301**:268–276 (2005).
20. D. Quintanar-Guerrero. Preparation techniques and mechanisms of formation of biodegradable nanoparticles from preformed polymers. *Drug Dev. Ind. Pharm* **24**:1113–1128 (1998).
21. P. Couvreur. Oral and parental administration of insulin associated to hydrolysable nanoparticles. *Acta Pharm. Technol* **26**:220 (1980).
22. A. Sze, D. Erickson, L. Ren, D. Li. Zeta-potential measurement using the Smoluchowski equation and the slope of the current–time relationship in electroosmotic flow. *J. Colloid Interf. Sci*. **26** (2):402–410 (2003).
23. M. Timothy, J. A. Crowder, J. D. Rosati, A. J. Schroeter, and T. B. Martonen. Fundamental effects of particle morphology on lung delivery: predictions of stokes' law and the particular relevance to dry powder inhaler formulation and development. *Pharm. Res*. **19**(3):239–245 (2004).